Photophysics of Pyridylporphyrin Ru(II) Adducts: Heavy-Atom Effects and Intramolecular Decay Pathways

Anna Prodi, Cornelis J. Kleverlaan, M. Teresa Indelli, and Franco Scandola*

Dipartimento di Chimica, Università di Ferrara, 44100 Ferrara, Italy

Enzo Alessio and Elisabetta Iengo

Dipartimento di Scienze Chimiche, Università di Trieste, Trieste 34127, Italy

Received January 31, 2001

Eight adducts between different pyridylporphyrins and ruthenium complexes, MPyP[$RuCl_2(DMSO)_2(CO)$], *c*-DPyP-[$RuCl_2(DMSO)_2(CO)]_2$, TrPyP[$RuCl_2(DMSO)_2(CO)]_3$, TPyP[$RuCl_2(DMSO)_2(CO)]_4$, $(MPyP)_2[RuCl_2(DMSO)_2]$, $\{c$-DPyP[$RuCl_2(DMSO)_2]\}_2$, MPyP[$RuCl_2(CO)_3$], and $\{c$-DPyP[$RuCl_2(CO)_2]\}_2$, have been investigated. The results show that in all the adducts the porphyrin singlet is quenched, to a greater or lesser extent, relative to the parent-free molecule. This study provides insight into the mechanisms of singlet quenching in the adducts. Two mechanisms for singlet quenching, both related to the "heavy-atom effect" of the ruthenium center and experimentally distinguishable by transient spectroscopy, are examined. Enhanced intersystem crossing within the porphyrin chromophore is demonstrated for the series of adducts MPyP[$RuCl_2(DMSO)_2(CO)$], *c*-DPyP[$RuCl_2(DMSO)_2$-$(CO)]_2$, TrPyP[$RuCl_2(DMSO)_2(CO)]_3$, and TPyP[$RuCl_2(DMSO)_2(CO)]_4$, where a nice correlation is observed between the magnitude of the effect and the number of ruthenium centers attached to the pyridylporphyrin chromophore. Singlet−triplet energy transfer from the pyridylporphyrin chromophore to the ruthenium center(s) is an additional efficient quenching channel for adducts containing ruthenium centers with weak field ligands and low triplet energies, such as $(MPyP)_2[RuCl_2(DMSO)_2]$ and $\{c$-DPyP[$RuCl_2(DMSO)_2]\}_2$.

Introduction

In the rapidly developing field of supramolecular chemistry,[1] porphyrins and metalloporphyrins occupy a relevant place, being frequently used as building blocks for the construction of artificial systems with special built-in properties or functions. Among these, light-induced functions[2] and in particular those inspired by natural photosynthesis have attracted a great deal of attention. Photoinduced charge separation in the reaction center[3] is mimicked by several types of covalently linked donor−acceptor systems, including porphyrin-based "triads" and more complex architectures.[4] For the light-harvesting function carried out by a large number of chlorophyll molecules in the "antenna" units,[5] several synthetic models have been developed, including multiporphyrin arrays.[6]

Pyridylporphyrins (PyPs) can be considered as particularly attractive building blocks for the construction of photoactive supramolecular systems. A typical series, carrying a variable number of 4′-pyridyl (n) and phenyl ($4 - n$) groups in the meso positions of the porphyrin ring, is shown in structures **1**−**5**. As for other porphyrins, they have attractive spectroscopic, redox, and photophysical properties. In addition, however, the presence of meso pyridyl groups provides further synthetic flexibility, as these groups can be coordinated to metal-containing fragments of various coordination numbers and geometries. Adducts obtained by peripheral coordination of pyridylporphyrins to singly unsaturated metal centers have shown new, interesting photophysical properties.[7,8] On the other hand, when polyunsaturated metal fragments are used to bridge two (or more)

(1) *Comprehensive Supramolecular Chemistry*; Atwood, J. L., Davies, J. E., MacNicol, D. D., Vögtle, F., Eds.; Pergamon: Oxford, 1996. (b) Lehn, J.-M. *Supramolecular Chemistry: Concepts and Perspectives*; VCH: Weinheim, 1995.

(2) Balzani, V.; Scandola, F. *Supramolecular Photochemistry*; Harwood: Chichester, UK, 1991. (b) Balzani, V.; Scandola, F. In *Comprehensive Supramolecular Chemistry*; Atwood, J. L., Davies, J. E. D., MacNicol, D. D., Vögtle, F., Reinhoudt, D. N., Eds.; Pergamon: Oxford, 1996; Vol. 10, p 687.

(3) Deisenhofer, J.; Epp, O.; Miki, K.; Huber, R.; Michel, H. *J. Mol. Biol.* **1984**, *180*, 385. (b) Chang, C.-H.; Tiede, D. M.; Tang, J.; Smith, U.; Norris, J.; Schiffer, M. *FEBS Lett.* **1986**, *205*, 82. (c) Allen, J. P.; Feher, G.; Yeates, T. O.; Komiya, H.; Rees, D. C. *Proc. Natl. Acad. Sci. U.S.A.* **1987**, *84*, 5730. (d) Deisenhofer, J.; Michel, H. *Angew. Chem., Int. Ed. Engl.* **1989**, *28*, 829. (e) Huber, R. *Angew. Chem., Int. Ed. Engl.* **1989**, *28*, 848.

(4) Wasielewski, M. R. *Chem. Rev.* **1992**, *92*, 435. (b) Harriman, A.; Sauvage, J. P. *Chem. Soc. Rev.* **1996**, 41. (c) Gust, D.; Moore, T. A.; Moore, A. L. *Acc. Chem. Res.* **1993**, *26*, 198.

(5) McDermott, G.; Prince, S. M.; Freer, A. A.; Hawthornthwaite-Lawless, A. M.; Papiz, M. Z.; Cogdell, R. J.; Isaacs, N. W. *Nature* **1995**, *374*, 517. (b) Kuhlbrandt, W. *Nature* **1995**, *374*, 497. (c) Karrasch, S.; Bullough, P. A.; Ghosh, R. *EMBO J.* **1995**, *14*, 631. (d) Kuhlbrandt, W.; Wang, D. N.; Fujiyoshi, Y. *Nature* **1994**, *367*, 1994. (e) Pullerits, T.; Sundström, V. *Acc. Chem. Res.* **1996**, *29*, 381.

(6) Anderson, S.; Anderson, H. L.; Bashall, A.; McPartlin, M.; Sanders, J. K. M. *Angew. Chem., Int. Ed. Engl.* **1995**, *34*, 1096. (b) Davila, J.; Harriman, A.; Milgrom, L. R. *Chem. Phys. Lett.* **1987**, *136*, 427. (c) Prathapan, S.; Johnson, T. E.; Lindsey, J. S. *J. Am. Chem. Soc.* **1993**, *115*, 7519. (d) Hsiao, J.-S.; Krueger, B. P.; Wagner, R. W.; Johnson, T. E.; Delaney, J. K.; Mauzerall, D. C.; Fleming, G. R.; Lindsey, J. S.; Bocian, D. F.; Donohoe, R. J. *J. Am. Chem. Soc.* **1996**, *118*, 11181. (e) Nakano, A.; Osuka, A.; Yamazaki, I.; Yamazaki, T.; Nishimura, Y. *Angew. Chem., Int. Ed.* **1998**, *37*, 3023. (f) Kuciauskas, D.; Liddell, P. A.; Lin, S.; Johnson, T. E.; Weghorn, S. J.; Lindsey, J. S.; Moore, A.; Moore, T. A.; Gust, D. *J. Am. Chem. Soc.* **1999**, *121*, 8604.

(7) Alessio, E.; Macchi, M.; Heath, S.; Marzilli, L. G. *Inorg. Chem.* **1997**, *36*, 5614.

(8) Toma, H. E.; Araki, K. *J. Photochem. Photobiol., A* **1994**, *83*, 245.

10.1021/ic0101331 CCC: $20.00
Published on Web 06/05/2001

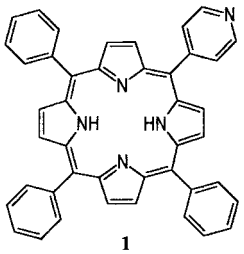

1
MPyP

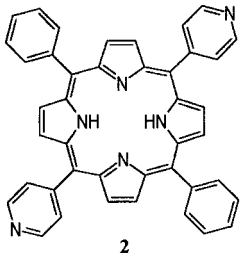

2
t-DPyP

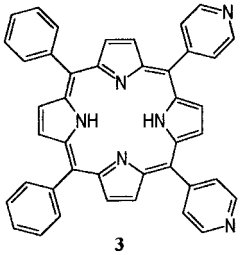

3
c-DPyP

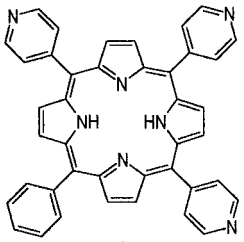

4
TrPyP

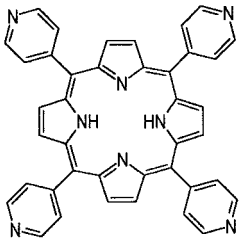

5
TPyP

pyridylporphyrin units, supramolecular species of considerable structural and photophysical interest, ranging from discrete supramolecules (molecular squares, 3×3 arrays)[9] to solid-state arrays (tapes, surfaces)[9e,10] are obtained.

Furthermore, when the peripheral pyridyl groups coordinate axially to the metal center of another porphyrin, interesting "side-to-face" porphyrin arrays are generated.[11−14] The photophysical properties of these pyridylporphyrin adducts have not always been investigated in detail. When this was done, however, the lifetime of the lowest singlet excited state and the associated fluorescence emission were always found to be substantially quenched in the metal adducts with respect to the free pyridylporphyrin chromophore.[9a−c,e,f,11d] This was true even for systems in which any obvious quenching mechanism between the chromophore and the metal-containing unit (e.g., singlet energy transfer, photoinduced electron transfer) could be ruled out. For example, in side-to-face adducts between pyridylporphyrins and ruthenium porphyrins such as **6** and **7**,[11d]

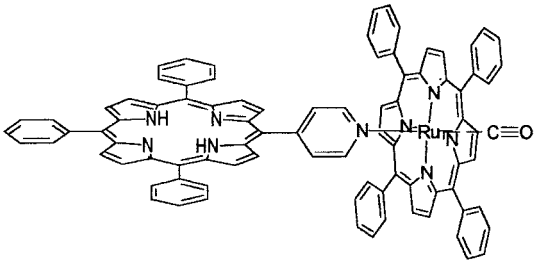

6
MPyP[Ru(TPP)CO]

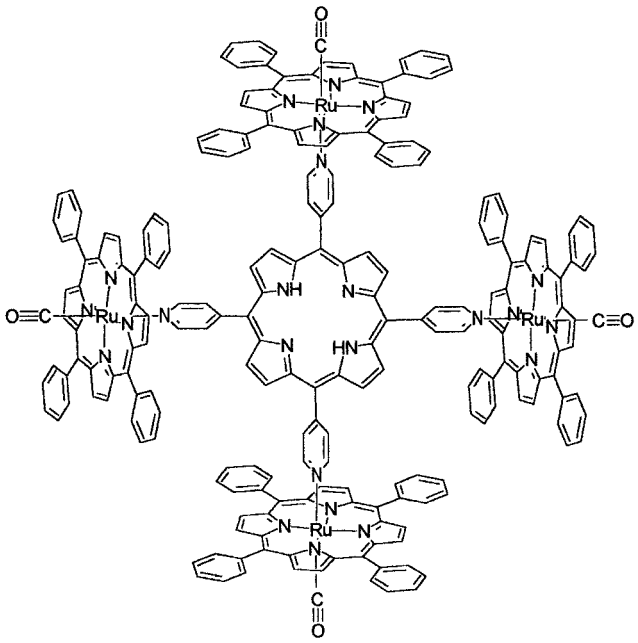

7
TPyP[Ru(TPP)CO]$_4$

the pyridylporphyrin singlet is definitely lower in energy than both the ruthenium porphyrin singlet state and the lowest intercomponent charge-transfer state. Nevertheless, the fluorescence lifetime of the pyridylporphyrin unit is much shorter in the dimer **6** (3.6 ns) and in the pentamer **7** (0.5 ns) than in the corresponding free pyridylporphyrins (e.g., 9.7 ns for MPyP). We[11d] and others[9a,e,f] suggested that the quenching of the singlet state of the pyridylporphyrin in the adducts is due to the "heavy-atom effect" of the metal.[15]

(9) Drain, C. M.; Lehn, J.-M. *J. Chem. Soc., Chem. Commun*. **1994**, 2313. (b) Yuan, H.; Thomas, L.; Woo, L. K. *Inorg. Chem*. **1996**, *35*, 2808. (c) Slone, R. V.; Hupp, J. T. *Inorg. Chem*. **1997**, *36*, 5422. (d) Stang, P. J.; Fan, J.; Olenyuk, B. *Chem. Commun*. **1997**, 1453. (e) Drain, C. M.; Nifiatis, F.; Vasenko, A.; Batteas, J. D. *Angew. Chem., Int. Ed.* **1998**, *37*, 2344. (f) Fan, J.; Whiteford, J. A.; Olenyuk, B.; Levin, M. D.; Stang, P. J.; Fleischer, E. B. *J. Am. Chem. Soc*. **1999**, *121*, 2741.

(10) Sharma, C. V. K.; Broker, G. A.; Huddleston, J. G.; Baldwin, J. W.; Metzger, R. M.; Rogers, R. D. *J. Am. Chem. Soc.* **1999**, *121*, 1137−1144. (b) Pan, L.; Nool, B. C.; Wang, X. *Chem. Commun.* **1999**, 157−158.

(11) Alessio, E.; Macchi, M.; Heath, S.; Marzilli, L. G. *Chem. Commun*. **1996**, 1411. (b) Alessio, E.; Geremia, S.; Mestroni, S.; Iengo, E.; Srnova, I.; Slouf, M. *Inorg. Chem*. **1999**, *38*, 869. (c) Alessio, E.; Geremia, S.; Mestroni, S.; Gianferrara, T.; Slouf, M.; Prodi, A. *Inorg. Chem.* **1999**, *38*, 2527. (d) Prodi, A.; Indelli, M. T.; Kleverlaan, C. J.; Scandola, F.; Alessio, E.; Gianferrara, T.; Marzilli, L. G. *Chem. Eur. J.* **1999**, *5*, 2668.

(12) Kimura, A.; Funatsu, K.; Imamura, T.; Kido, H.; Sasaki, Y. *Chem Lett*. **1995**, 207. (b) Funatsu, K.; Kimura, A.; Imamura, T.; Sasaki, Y. *Chem Lett.* **1995**, 765. (c) Kariya, N.; Imamura, T.; Sasaki, Y. *Inorg. Chem*. **1997**, *36*, 833. (d) Funatsu, K.; Kimura, A.; Imamura, T.; Ichimura, A.; Sasaki, Y. *Inorg. Chem*. **1997**, *36*, 1625. (e) Kariya, N.; Imamura, T.; Sasaki, Y. *Inorg. Chem*. **1998**, *37*, 1658. (f) Funatsu, K.; Imamura, T.; Ichimura, A.; Sasaki, Y. *Inorg. Chem*. **1998**, *37*, 1798.

(13) Darling, S. I.; Mak, C. C.; Bampos, N.; Feeder, N.; Teat, S. J.; Sanders, J. K. *New J. Chem*. **1999**, *23*, 359. (b) Mak, C. C.; Bampos, N.; Sanders, J. K. *Chem. Commun*. **1999**, 1085.

(14) Krishna, Kumar; Goldberg, R. I. *Angew. Chem., Int. Ed.* **1998**, *37*, 3027−3030.

(15) In most of these studies, the metal centers involved were 4d or 5d metals [e.g., Ru(II), Pd(II), Re(I), and Pt(II)]. Aside from synthetic and stability reasons, this is motivated by the need to avoid low-lying metal-centered excited states acting as radiationless deactivation sinks.

The conventional notion of this effect is that the presence of heavy atoms provides a spin−orbit coupling perturbation, thereby relaxing the spin-selection rules for radiative and radiationless transitions. In a simple molecular system, quenching of the lowest excited singlet state (S_1) in the presence of a heavy atom is expected, a consequence of enhanced intersystem crossing ($S_1 \rightarrow T_1$). The situation is more complex for a supramolecular system, where excited states localized on different molecular components are present. In such a case, both intra- and intercomponent spin-forbidden processes could, in principle, be responsible for the observed quenching effect (see Discussion). To obtain further insight into the heavy-atom effect in such supramolecular systems, we have now studied in some detail the photophysical behavior of the series of adducts **8**−**15**.

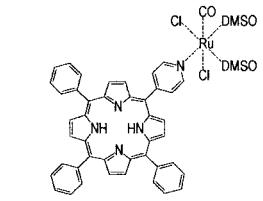

8
MPyP[$RuCl_2(DMSO)_2(CO)$]

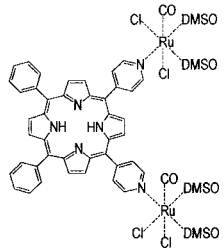

9
c-DPyP[$RuCl_2(DMSO)_2(CO)]_2$

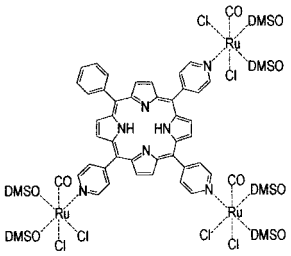

10
TrPyP[$RuCl_2(DMSO)_2(CO)]_3$

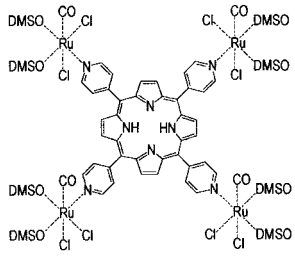

11
TPyP[$RuCl_2(DMSO)_2(CO)]_4$

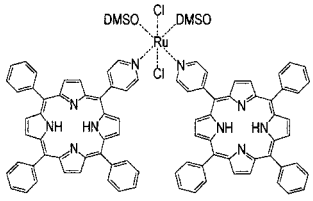

12
$(MPyP)_2[RuCl_2(DMSO)_2]$

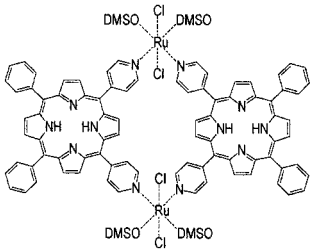

13
$\{c\text{-DPyP}[RuCl_2(DMSO)_2]\}_2$

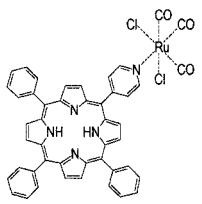

14
MPyP[$RuCl_2(CO)_3$]

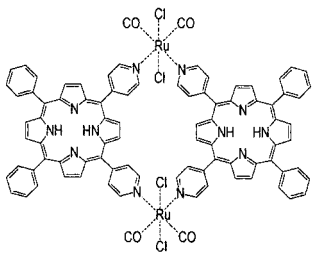

15
$\{c\text{-DPyP}[RuCl_2(CO)_2]\}_2$

They involve four pyridylporphyrins (**1** and **3**−**5**) and four octahedral Ru(II) fragments differing in ligands and stereochemistry (see model molecules **I**−**IV**).

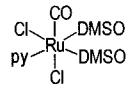

I
cis,cis,cis-$RuCl_2(DMSO)_2(CO)(py)$

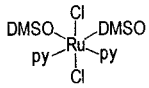

II
trans,cis-$RuCl_2(DMSO)_2(py)_2$

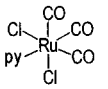

III
cis,fac-$RuCl_2(CO)_3(py)$

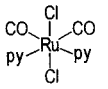

IV
trans,cis-$RuCl_2(CO)_2(py)_2$

Experimental Section

Materials. The syntheses and full NMR characterizations of adducts **8**, **9**, **11**, and **12** and model compounds **I**, **III**, and **IV**[16] are reported elsewhere; the preparation and full spectroscopic characterization of **13** and **15** are being described elsewhere.[17] The synthesis and characterization of adducts **10** and **14** and model compound **II** are reported herein.

TrPyP[$RuCl_2(DMSO)_2(CO)]_3$ (10). A 182.6-mg amount of *cis*,*fac*-$RuCl_2(DMSO)_3(CO)$ (0.42 mmol) was added to a solution of TrPyP·0.5$CHCl_3$ (81.2 mg, 0.12 mmol) in 15 mL of $CHCl_3$, and the mixture reacted for 24 h at room temperature. The product precipitated as a noncrystalline, purple solid after the solution was concentrated to less than half of its volume (without heating) and diethyl ether was added; it was collected by filtration, washed with cold acetone and diethyl ether, and vacuum-dried. Yield: 65%. Anal. Calcd for $C_{56}H_{63}N_7Cl_6O_9Ru_3S_6$ (MW = 1686.46): C, 39.9; H, 3.77; N, 5.81. Found: C, 39.2; H, 3.65; N, 5.87. mp >300 °C. ^{1}H NMR ($CDCl_3$, 400 MHz, 25 °C): −2.93 (2, s, NH), 3.61 (9, s, DMSO), 3.64 (9, s, DMSO), 3.69 (18, s, DMSO), 7.80 (3, m, *m*+*p*H), 8.17 (2, m, *o*H), 8.22 (6, m, H3,5), 8.87 (2, m, *β*H), 8.93 (6, m, *β*H), 9.50 (6, m, H2,6). Selected IR bands (Nujol, cm^{-1}): $\nu_{C=O}$ = 1982 (vs); $\nu_{S=O}$ = 1110 (vs).

MPyP[$RuCl_2(CO)_3$] (14). A 50-mg amount of *cis*,*fac*-$RuCl_2(CO)_3$(DMSO) (0.15 mmol) was added to a solution of MPyP·0.5$CHCl_3$ (81.2 mg, 0.12 mmol) in 10 mL of $CHCl_3$, and the mixture reacted for 24 h at room temperature. The product precipitated as a noncrystalline, purple solid after the solution was concentrated to less than half of its volume (without heating), and diethyl ether was added; it was collected by filtration, washed with cold acetone and diethyl ether, and vacuum-dried. Yield: 74 mg (70%). Anal. Calcd for $C_{46}H_{29}N_5Cl_2O_3Ru$ (MW = 871.73): C, 63.4; H, 3.35; N, 8.03. Found: C, 64.0; H, 3.28; N, 7.89. mp >300 °C. ^{1}H NMR ($CDCl_3$, 400 MHz, 25 °C): −2.77 (2, s, NH), 7.78 (9, m, *m*+*p*H), 8.22 (6, m, *o*H), 8.41 (2, d, J = 8 Hz, H3,5), 8.87 (6, m, *β*H), 8.94 (2, d, *β*H), 9.36 (2, d, J = 8 Hz, H2,6). Selected IR bands (Nujol, cm^{-1}): $\nu_{C=O}$ = 2135, 2070, 1995 (vs).

***trans,cis*-$RuCl_2(DMSO)_2(py)_2$ (II).** Pyridine (85 μL, 1 mmol) was added to a solution of 0.2 g of *trans*-$RuCl_2(DMSO)_4$ (0.41 mmol) in 8 mL of chloroform, and the mixture reacted overnight at room temperature. The solution was then concentrated in vacuo to ca. 2 mL and stored at 4 °C after a few drops of diethyl ether were added. Deep yellow microcrystals of the product formed within 24 h and were removed by filtration, washed with diethyl ether, and vacuum-dried. Yield: 0.18 g (90%). Anal. Calcd for $C_{14}H_{22}Cl_2N_2O_2RuS_2$ (MW = 486.45): C, 34.6; H, 4.59; N, 5.76. Found: C, 34.4; H, 4.65; N, 5.64. ^{1}H NMR ($CDCl_3$, 400 MHz, 25 °C): 3.26 (12, s, DMSO), 7.24 (2, m, *p*H), 7.72 (4, m, *m*H), 9.15 (4, m, *o*H). The solvents for the spectroscopic measurements, dichloromethane (CH_2Cl_2), ethanol (EtOH), and butyronitrile were of spectroscopy grade and used as received.

Apparatus. NMR spectra, recorded in $CDCl_3$ on a JEOL EX400 spectrometer, were referenced to residual $CHCl_3$ (δ = 7.26). UV−vis

(16) Alessio, E.; Milani, B.; Bolle, M.; Mestroni, G.; Faleschini, P.; Todone, F.; Geremia, S.; Calligaris, M. *Inorg. Chem.* **1995**, *34*, 4722−4734.
(17) Iengo, E.; Minatel, R.; Zangrando, E.; Alessio; E. Manuscript in preparation.

spectra were recorded with a Perkin-Elmer LAMBDA40 spectrophotometer. Emission spectra were taken on a Spex Fluoromax-2 or on a Perkin-Elmer MPF 44E spectrofluorimeter (77 K measurements), equipped with Hamamatsu R3896 tubes.

Nanosecond flash photolysis was performed by irradiating the sample with 6−8-ns full width at half-maximum pulses of a Continuum Surelight II Nd:YAG laser (10 Hz repetition rate) using a pulsed Xe lamp perpendicular to the laser beam as probing light. The desired excitation wavelength was obtained by frequency doubling (532 nm). The 150 W Xe lamp was equipped with an Applied Photophysics model 40 power supply and Applied Photophysics model 410 pulsing unit (giving pulses of 2 ms). A shutter, Oriel model 71445, placed between the lamp and the sample was opened for 100 ms to prevent PMT fatigue and photodecomposition. Suitable pre- and postcutoff and band-pass filters were used to prevent photodecomposition and scatter light of the laser. The light was collected in a LDC Analytical monochromator, detected by a R928 PMT (Hamamatsu), and recorded on a Lecroy 9360 (600 MHz) oscilloscope. The laser oscillator, Q-switch, lamp, shutter, and trigger were externally controlled with a digital logic circuit, which allowed for synchronous timing. The absorption transient decays were plotted as $\Delta A = \log(I_o/I_t)$ vs time, where I_o was the monitoring light intensity prior to the laser pulse, and I_t was the observed signal observed at delay time t. Transient spectra were obtained from the decays measured at various wavelengths, sampling the absorbance changes at constant delay time.

Emission lifetimes were measured by time-correlated single-photon counting using a PRA 3000 nanosecond fluorescence spectrometer equipped with a model 510B nanosecond pulsed lamp and a model 1551 cooled photomultiplier; the data were collected on a Tracor Northern multichannel analyzer and processed using original Edinburgh Instruments software.

Electrochemical measurements were carried out with a PC interfaced Eco Chemie Autolab/Pgstat30 Potentiostat, using the General Purpose Electrochemical System (GPES), version 4.7 software. All the low-temperature experiments were measured by using an Oxford Instruments DN 704 cryostatic equipment with quartz windows and a standard 1-cm spectrofluorimetric cuvette.

Procedures. Cyclic voltammetric measurements were carried out on Argon-purged 10^{-3} M sample solutions in CH_2Cl_2 (Romil, Hi-dry), containing 0.1 M [TBA]PF_6 (Fluka, electrochemical grade, 99%; dried in an oven). A conventional three-electrode cell assembly was used in CV: a saturated calomel electrode (SCE, $\varnothing = 6$ mm, AMEL) and a platinum wire, both separated from test solution by a frit, were used as reference and counter electrodes, respectively; a glassy carbon electrode (8 mm^2, AMEL) was used as a working electrode. Cyclic voltammograms were recorded at room temperature, in a potential window ranging from −2 to +1.7 V vs SCE and were appreciably independent of different scan rates in the range 20−1000 mV/s. Reported data will be referred to at a 100 mV/s scan rate. For reversible processes, the halfwave potential value was calculated from the average of the potential value of cathodic and anodic peaks with an experimental error within ±0.02 V.

Fluorescence decay measurements were performed with 3×10^{-5} M solutions by time-correlated single-photon counting. Time profiles were analyzed with standard iterative nonlinear procedures according to single exponentials ($0.98 \leq \chi^2 \leq 1.08$; estimated error on the lifetime = ±0.1 ns).

Results

Stability in Solution. As shown by previous work on side-to-face porphyrin arrays, the stability of pyridylporphyrin adducts may be a critical issue. Although the high affinity of Ru−dimethyl sulfoxide complexes for N-donor ligands[18] is likely to make the present adducts more stable than the previously described multiporphyrin arrays,[10d] similar precautions were taken to avoid the use of coordinating solvents and extremely diluted solutions. The experiments reported in this paper refer to solutions in dichloromethane at concentrations higher than 1×10^{-5} M, unless otherwise noted. In these conditions, no appreciable dissociation was revealed by concentration-dependent spectrophotometric measurements. The solutions were also photochemically stable. In particular, no decomposition was observed during the laser flash photolysis experiments.

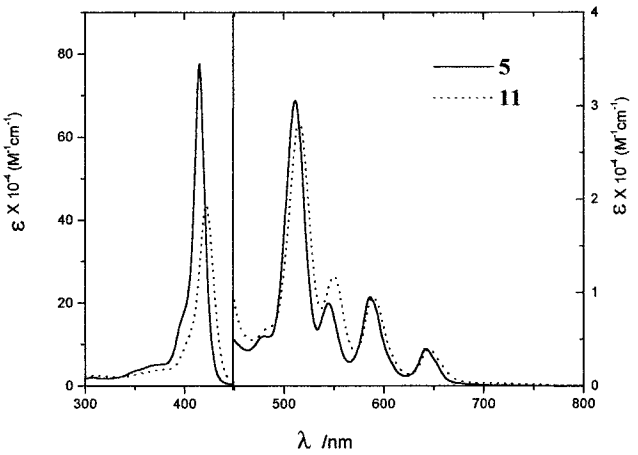

Figure 1. Absorption spectra of **5** (full line) and adduct **11** (dotted line) in CH_2Cl_2.

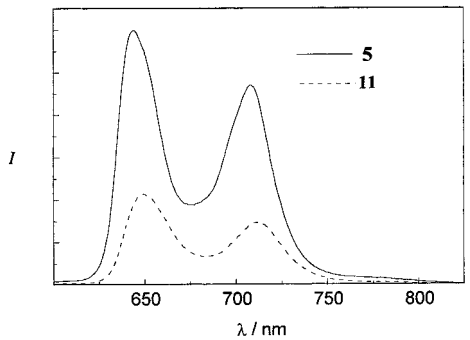

Figure 2. Emission spectra of **5** (full line) and adduct **11 (**dotted line) in CH_2Cl_2; optically matched solutions (excitation wavelength, 590 nm).

Absorption Spectra. The absorption spectrum of TPyP-$[RuCl_2(DMSO)_2(CO)]_4$ (**11**) is shown in Figure 1. The spectra of all the other adducts (**8**−**15**) were practically identical to that of Figure 1, with very minor changes (±2 nm) in the wavelength of absorption maxima. The spectra of the adducts were in all cases very similar, except for a small bathochromic shift (2−6 nm), to those[11d] of the parent pyridylporphyrins. The fact that the spectra of the adducts are dominated by the pyridylporphyrin component is consistent with the very small visible absorption expected from the Ru(II) components. For instance, *trans*,*cis*,*cis*-$RuCl_2(DMSO)_2(py)_2$ (**II**, appropriate model for adducts **12** and **13**) has a weak d−d band at 430 nm, and *cis*,*cis*,*cis*-$RuCl_2(DMSO)_2(CO)py$ (**I**, appropriate model for adducts **8**−**11**) only starts absorbing at 380 nm.

Emission. All the pyridylporphyrins exhibit strong fluorescence (Φ, ca. 0.1) with very similar emission spectra (±2 nm). That of **5**, TPyP (λ_{max} = 644, 709 nm), is shown in Figure 2. For purposes of comparison (see Discussion), the emission spectrum of the methylpyridinium analogue, $TMePyP^{4+}$, was also studied. The relevant data, in EtOH, are as follows: $TMePyP^{4+}$, λ_{max} = 653, 716 nm; TPyP, λ_{max} = 645, 711 nm.

In contrast, ruthenium model compounds, e.g., **I** and **II** , do not emit either at room temperature or at 77 K (butyronitrile

(18) Henn, M.; Alessio, E.; Mestroni, G.; Calligaris, M.; Attia, W. M. *Inorg. Chim. Acta* **1991**, *187*, 39. (b) Iwamoto, M.; Alessio, E.; Marzilli, L. G. *Inorg. Chem.* **1996**, *35*, 2384. (c) Alessio, E.; Calligaris, M.; Iwamoto, M.; Marzilli, L. G. *Inorg. Chem.* **1996**, *35*, 2538.

Table 1. Fluorescence Lifetimes of Pyridylporphyrins and Adducts[a]

no.	molecule	(τ, ns)[b]	(τ^0/τ)[c]
1	MpyP	8.1	
3	*c*-DPyP	8.0	
4	TrPyP	7.5	
5	TPyP	7.1; 9.1[d]	
	$TMePyP^{4+}$	10.1[d]	
8	$MPyP[RuCl_2(DMSO)_2(CO)]$	6.3	1.29
9	$c\text{-}DPyP[RuCl_2(DMSO)_2(CO)]_2$	4.4	1.82
10	$TrPyP[RuCl_2(DMSO)_2(CO)]_3$	3.3	2.27
11	$TPyP[RuCl_2(DMSO)_2(CO)]_4$	2.7	2.63
12	$(MPyP)_2[RuCl_2(DMSO)_2]$	4.8	1.69
13	$\{c\text{-}DPyP[RuCl_2(DMSO)_2]\}_2$	2.2	3.64
14	$MPyP[RuCl_2(CO)_3]$	6.7	1.21
15	$\{c\text{-}DPyP[RuCl_2(CO)_2]\}_2$	5.7	1.40

[a] In CH_2Cl_2, unless otherwise noted. [b] Estimated error, ± 0.1 ns. [c] For definition of τ^0, see Discussion. [d] In EtOH.

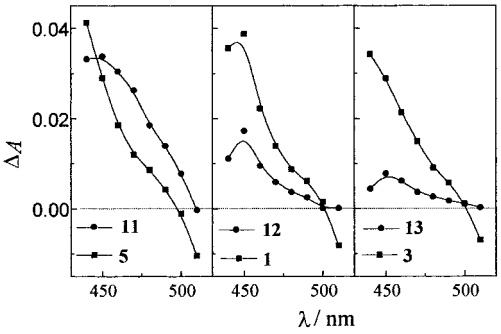

Figure 3. Transient absorption spectra of pyridylporphyrins and adducts: **5** and **11**, **1** and **12**, and **3** and **13**. Isoabsorptive solutions of porphyrin and adduct (at the excitation wavelength, 355 nm); spectra taken 20 ns after pulsed laser excitation.

glass), as expected for Ru(II) complexes with the lowest d−d states.[19]

All the pyridylporphyrin−Ru(II) adducts exhibit fluorescent emissions with very similar maxima, except for a small red shift ($\leq$10 nm) to their parent pyridylporphyrins. The emission spectrum of **11** (λ_{max} = 650, 712 nm) is compared with that of the parent pyridylporphyrin (**5**) in Figure 2. Since the spectra were obtained on optically matched (at the excitation wavelength) solutions, Figure 2 also emphasizes the fact that the emission of the adduct is weaker than that of the parent pyridylporphyrin. This was true, to a varying degree, for all the adducts examined. The differences in emission intensity between the various species are paralleled, as expected, by differences in emission lifetimes. Lifetimes for pyridylporphyrins and adducts are collected in Table 1. For purposes of comparison (see Discussion), the lifetime of the methylpyridinium analogue of TPyP, $TMePyP^{4+}$, has also been included.

Transient Absorption. Transient spectra were measured using deareated solutions, in the spectral range 440−510 nm, where the triplet states of the pyridylporphyrins exhibit distinct absorption.[11d] Figure 3 shows the difference spectra obtained for adducts **11** $TPyP[RuCl_2(DMSO)_2(CO)]_4$, **12** $(MPyP)_2[RuCl_2(DMSO)_2]$, and **13** $\{c\text{-}DPyP[RuCl_2(DMSO)_2]\}_2$. These transient spectra are compared with those obtained for isoabsorptive (at the excitation wavelength) solutions of the appropriate parent pyridylporphyrins (**5**, TPyP; **1**, MPyP; and **3**, *c*-DPyP, respectively). All the transient spectra were taken 20 ns after pulsed laser excitation (at 355 nm) and remained appreciably constant in a microsecond time scale.

(19) Ford, P. C.; Wink, D.; Di Benedetto, J. *Prog. Inorg. Chem.* **1983**, *30*, 213.

Table 2. First Oxidation and Reduction Processes of Selected Adducts[a]

no.	adduct	E_{red},[b] *V* vs SCE	E_{ox},[c] *V* vs SCE	$\Delta E_{ox/red} - w_p$,[d] *V*
8	$MPyP[RuCl_2(DMSO)_2(CO)]$	-1.22	1.05	2.11
11	$TPyP[RuCl_2(DMSO)_2(CO)]_4$	-0.91	1.04	1.79
12	$(MPyP)_2[RuCl_2(DMSO)_2]$	-1.17	1.04	2.04
13	$\{c\text{-}DPyP[RuCl_2(DMSO)_2]\}_2$	-1.10	1.04	1.98
15	$\{c\text{-}DPyP[RuCl_2(CO)_2]\}_2$	-1.07	1.02	1.93

[a] All measurements were made in CH_2Cl_2 containing 0.1 M $[TBA]PF_6$ with a scan rate of 100 mV/s; all potentials are vs SCE, and the ferrocenium−ferrocene couple was used as an internal reference (0.43 $\pm$ 0.02 V). [b] Halfwave potential in cyclic voltammetry (ΔE = 80−100 mV). [c] Halfwave potential in cyclic voltammetry (ΔE = 60−70 mV). [d] Estimated energy of electron-transfer state, see Discussion.

Table 3. Numbering Scheme of Porphyrin Models for Adducts and Constituent Units

	Ru-containing unit			
	I	**II**	**III**	**IV**
1	**8**	**12**	**14**	
2	**9**	**13**		**15**
4	**10**			
5	**11**			

Redox Potentials. A complete characterization of the electrochemical behavior of model systems and adducts was not attempted. For mechanistic reasons (see Discussion), attention was focused on the potential values for the first oxidation and reduction processes. Values for a number of pyridylporphyrin−Ru(II) adducts are reported in Table 2. In all the adducts, the first reduction process takes place at the porphyrin ring (in Ru(II) model compounds **I** and **II**, reduction only occurs at potentials more negative than −1.50 V). The assignment of the first oxidation process is uncertain, as both the pyridylporphyrins and the Ru(II) models undergo oxidation in the same potential range (0.98−1.07 V).

Discussion

To facilitate the discussion of the photophysical effects observed upon adduct formation, Table 3 summarizes the relationships between the adducts (**8**−**15**), the parent pyridylporphyrins (**1**, **2**, **4**, **5**), and the ruthenium-containing units (**I**−**IV**). Inspection of Table 1 reveals that in all the adducts the emitting singlet excited state is shorter lived than in the parent pyridylporphyrin molecule. The differences are not very large but clearly outside the experimental error ($\pm$0.1 ns). The ratios between the lifetimes of parent pyridylporphyrin, τ^0, and adduct, τ, are given in the last column of Table 1 and are plotted in Figure 4 as a function of the number of ruthenium centers attached to each pyridylporphyrin chromophore. The interesting observations are as follows: (i) With the same type of Ru center, there is a nice correlation between the lifetime shortening and the number of metal centers attached to each chromophore (e.g., adducts **8**−**11** and adducts **12** and **13**). (ii) The magnitude of the effect seems to depend markedly on the nature of the Ru center (**II** > **I** > **IV** $\approx$ **III**).

A preliminary question to be answered is whether the decrease in fluorescence lifetime after adduct formation could be a consequence of coordination as such. As a matter of fact, some perturbation of the energy levels of the porphyrin chromophore takes place after adduct formation, as shown by the ubiquitous, though small, red shift of fluorescence. That these energy changes do not cause, per se, fluorescence quenching is demonstrated by the comparison between **5** and the analogous

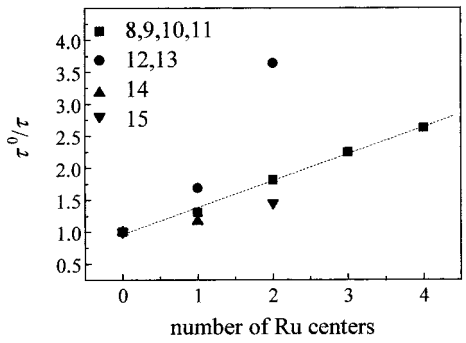

Figure 4. Trends in porphyrin singlet quenching after adduct formation. The extent of quenching, given as the ratio of the fluorescence lifetime of the parent pyridylporphyrin (τ^0) to that of the adduct (τ), is plotted as a function of the number of ruthenium centers attached to each pyridylporphyrin.

N-methylpyridinium species $TMePyP^{4+}$. This species can be taken as a model for TPyP interacting with a strong Lewis acid. The results show that methylation of the pyridyl nitrogens is indeed accompanied by a pronounced red shift of the fluorescence. The lifetime, however, is hardly affected (in fact, a small increase is observed in Table 1). Thus, the fluorescence quenching generally observed in the adducts should be attributed to intrinsic properties of the metal-containing fragments other than their Lewis acid behavior.

As far as potential-quenching mechanisms are concerned, singlet−singlet energy transfer can be easily ruled out on energetic grounds. The appended Ru(II) units do not show appreciable absorption at $\lambda \geq 500$ nm, implying that their lowest singlet states (of metal-centered nature) are always much higher ($\geq$4600 cm^{-1}) than the porphyrin singlet.

Intramolecular ruthenium-to-porphyrin electron transfer is another potential mechanism for the quenching of the porphyrin excited singlet state. In principle, the energy of the relevant electron-transfer state can be inferred from electrochemical data. To do this, the difference between the first oxidation and the reduction potentials must be corrected to account for the Coulombic stabilization[20] (ca. 0.16 V) of the electron-transfer state (Table 2). The singlet excited-state energy of the porphyrin unit in this series of adducts is 1.92 ± 0.02 eV. Inspection of Table 2 shows that conversion to the electron-transfer state would be clearly uphill for **8**, **12**, and **13**; slightly endoergonic for **15**; and downhill only for **11**. However, there is no apparent correlation between the electron-transfer energy in Table 2 (**8** > **12** > **13** > **15** > **11**) and the quenching efficiency in Table 1 (**8** < **15** < **12** < **11** < **13**). Thus, although some contribution cannot be definitely ruled out (especially for **11**), intramolecular electron transfer does not seem to be a likely quenching pathway for this series of adducts.

The heavy-atom effect was suggested as an effective singlet-quenching mechanism in previously studied porphyrin arrays containing pyridylporphyrin and Ru(II) units (**6** and **7**).[11d] In broad terms, this effect refers to the enhancement, by spin−orbit coupling, of a formally spin-forbidden deactivation process of the singlet state of the porphyrin. It is important to realize that, in supramolecular systems of this type, two spin-forbidden deactivation channels are generally available to the porphyrin singlet (Figure 5): (i) intersystem crossing within the porphyrin chromophore (k_{ISC}) and (ii) singlet−triplet energy transfer to the attached unit (k_{STEn}).[21] In principle, both channels can become partially allowed as a consequence of the heavy-atom

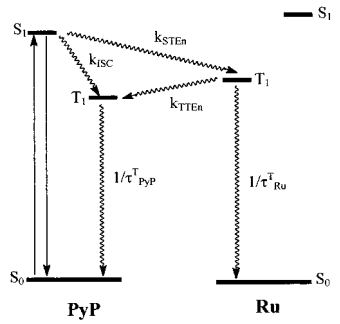

Figure 5. Schematic representation of the deactivation pathways from the porphyrin singlet excited state in the adducts (PyP, pyridylporphyrin unit; Ru, ruthenium complex unit).

effect of ruthenium. Their relative importance is difficult to predict. For k_{ISC}, the heavy atom is remote, but the process is an intracomponent one. For k_{STEn}, the heavy metal center is directly involved, but the process is an intercomponent one. Furthermore, the feasibility of k_{STEn} depends critically on the energy of the triplet state of the Ru(II) center.

In principle, transient spectroscopic experiments can be used to discriminate between the two pathways. An acceleration of the ISC process in the PyP−Ru adducts should not appreciably modify the amount of $PyP(T_1)$ formed with respect to the pyridylporphyrin models, where the quantum yield is already ca. 90%.[22] On the other hand, the yield of formation of $PyP(T_1)$ is expected to be substantially diminished if STEn takes place in the adducts, as the very short lifetime of the $Ru(T_1)$ states precludes any possibility of reformation of $PyP(T_1)$ by TTEn.[23] For three cases of substantial singlet quenching, pyridylporphyrin and adduct transient spectra are compared in Figure 3.

The results of Figure 3 seem to indicate different pathways for adducts with different Ru centers. In particular, for **11**, the $PyP(T_1)$ absorption has the same intensity (except for the expected red shift)[24] as for the pyridylporphyrin model **5**. This supports the acceleration of intersystem crossing within the porphyrin (k_{ISC} in Figure 5) after adduct formation. On the other hand, an evident decrease in triplet formation is observed for **12** and **13**,with the effect paralleling the amount of singlet quenching (Table 1 and Figure 4). This supports the occurrence, for this type of adduct, of singlet−triplet energy transfer (k_{STEn} in Figure 5).[25] Thus, both mechanisms seem to be operative in the adducts studied, the choice being dependent on the type of Ru center: enhanced intersystem crossing with centers of type **I** or singlet−triplet energy transfer with centers of type **II**. The

(20) Rehm, D.; Weller, A. *Ber. Bunsen-Ges. Phys. Chem.* **1969**, *73*, 834. (b) Weller, A. *Z. Phys. Chem.* **1982**, *133*, 93.

(21) These two quenching mechanisms are also mentioned by Mak, C. C.; Bampos, N.; Darling, S. L.; Montalti, M.; Prodi, L.; Sanders, J. K. M. *J. Org. Chem*. In press.

(22) Kalyanasundaram, K. *Inorg. Chem.* **1984**, *23*, 2453. (b) Kalyanasundaram, K. *Photochemistry of Polypyridine and Porphyrin Complexes*; Academic Press: London, 1992.

(23) This diagnostic possibility was not available for the previously studied Ru(II)−pyridylporphyrin arrays **6**−**7**,[11d] where the $Ru(T_1)$ states were intrinsically long-lived and efficient TTEn was observed.

(24) Analogous red shifts in triplet absorption were observed for side-to-face Ru(II)−pyridylporphyrin arrays.[11d] We have no reasons to believe that such shifts in the triplet−triplet absorption are accompanied by major changes in molar absorptivity.

(25) Exciton interaction could be suggested as an alternative quenching mechanism for bis-porphyrin adducts with cis geometry such as **12** and **13** (we thank one of the reviewers for pointing out this possibility). We could not find, however, any experimental indication of exciton coupling (e.g., spectral splittings) in these species. Furthermore, exciton quenching is ruled out by the fact that the bis-porphyrin adduct **15**, with exactly the same porphyrin geometry, is quenched to a much smaller extent than **13.**

most likely explanation for this switch in mechanism lies in the dependence of the energy of the $Ru(T_1)$ state on the coordination environment at the ruthenium center. Unfortunately, direct spectroscopic information on ligand-field triplet energies of this type of Ru(II) complex is not available. However, these energies depend on the average ligand field strength and are expected to decrease from **I** to **II** (CO > py). Thus, it is likely that the singlet−triplet energy transfer channel is energetically available for adducts containing ruthenium centers of type **II** (**12** and **13**) but not for adducts containing ruthenium centers of type **I** (**8**−**11**). The singlet−triplet energy transfer channel should be unavailable, a fortiori, for the adducts with ruthenium centers **III** (**14**) and **IV** (**15**) containing three and two strong-field CO ligands, respectively. Indeed, these adducts exhibit very similar quenching behavior, as far as we can tell from Figure 4, to those with type **I** ruthenium centers.

Conclusions

Eight different adducts between pyridylporphyrins and ruthenium complexes have been investigated. The results add to previous observations, showing that quenching of the porphyrin singlet is a general feature for these types of adducts. Furthermore, this study provides insight into the mechanisms of singlet quenching in the adducts. Two mechanisms are possible, both related to the relaxation of spin selection rules for singlet radiationless decay within the adduct. The two quenching mechanisms can be experimentally distinguished by means of transient spectroscopy.

The first mechanism is enhanced intersystem crossing within the porphyrin as a consequence of the heavy-atom effect of the ruthenium metal. This classical heavy-atom-induced quenching is expected to be a general phenomenon for ruthenium−pyridylporphyrin adducts. In a series of adducts of varying stoichiometry, its magnitude is found to correlate nicely with the number of ruthenium centers attached to the pyridylporphyrin chromophore.

A second quenching mechanism is singlet−triplet energy transfer between the pyridylporphyrin chromophore and the ruthenium centers. When energetically allowed, this mechanism provides an additional, efficient channel for singlet quenching. In the series of adducts studied, this mechanism seems to be limited to ruthenium centers with weak field ligands (and thus with low triplet energies).

Acknowledgment. This work was carried out with financial support from MURST (Progetto Fotosintesi Artificiale), CNR (Centro di Fotoreattività e Catalisi, Ferrara), EEC (TMRX-CT96-0076), and EU COST (Action D11, Supramolecular Chemistry, Project D11/0004/98).

IC0101331